

ORIGINAL RESEARCH PAPER

## Simultaneous loading of 5-flourouracil and SPIONs in HSA nanoparticles: Optimization of preparation, characterization and *in vitro* drug release study

<sup>1</sup>H. Kouchakzadeh; <sup>2</sup>S. Hoseini Makarem; <sup>2\*</sup>S.A. Shojaosadati

<sup>1</sup>Protein Research Center, Shahaid Behashti University, Tehran, Iran

<sup>2</sup>Biotechnology Group, Chemical Engineering Faculty, Tarbiat Modares University, Tehran, Iran

Received; 25 August 2015

Accepted; 5 November 2015

### ABSTRACT

**Objective(s):** Over the past two decades, considerable interest has been focused on utilizing biocompatible magnetic nanoparticles (MNPs) for biomedical applications. In this study, production of human serum albumin (HSA) nanoparticles using desolvation technique that were simultaneous loaded with high amounts of superparamagnetic iron oxide nanoparticles (SPIONs) and 5-flourouracil (5-FU) was investigated.

**Materials and Methods:** 5-FU loading (%) and SPIONs entrapment efficiency (%) were optimized using response surface methodology (RSM). The design expert software used to analyse the interactive effects of pH, 5-FU and SPIONs concentrations.

**Results:** The optimum conditions found to be pH of 8.2, drug concentration of 1.5 mg/ml and SPIONs concentration of 2.79 mg/ml. Under the mentioned optimum conditions, particles with the size of 111.8 nm, zeta potential of -37.1 mV, 5-FU loading of 15.8% and SPIONs entrapment efficiency of 41.1% were obtained. *In vitro* cumulative release of 5-FU from the nanoparticles was evaluated in phosphate buffer saline (pH 7.4, 37 °C). Results indicated that 85% of the 5-FU released during 95 h, which revealed a sustained release profile. In addition, Vibrating Sample Magnetometer (VSM) analyses confirmed the superparamagnetic properties of magnetic albumin nanoparticles manufactured under the optimum conditions.

**Conclusion:** According to the findings, SPIONs and 5-FU loaded HAS nanoparticles are promising for use as novel targeted delivery system due to proper magnetic and drug release behaviours.

**Keywords:** 5-Flourouracil, HSA nanoparticle, *In-vitro* drug release, Magnetic nanoparticle, Response surface methodology

### INTRODUCTION

Magnetic nanoparticles (MNPs) are nanoscale materials, which are able to overturn the theranostic techniques. Due to their unique properties, they can be manipulated at the cellular and molecular level of biological interactions [1]. Magnetic resonance imaging (MRI) [2, 3], hyperthermia of cancerous cells [4, 5], and targeted delivery of drugs for cancer treatment [3, 6] are some of the versatile usages of superparamagnetic iron oxide nanoparticles (SPIONs) in biomedical and clinical applications. In recent decades, nanoparticulate systems are playing an important role in targeted delivery of therapeutics.

Magnetic targeting has been proposed and used to increase the concentration of cytotoxic agents at their site of action since 30 years ago [6]. Despite the advantages of iron oxide nanoparticles, their direct clinical use may cause biofouling of the particles in the blood plasma. Consequently, cells of the reticuloendothelial system (RES) such as macrophages capture the aggregates and hinder their efficiency. To prevent and refuse this happening, SPIONs can be coated, entrapped or folded in biocompatible and biodegradable agents like polymers, liposome, and proteins. Among them, nanoparticulate systems based on proteins have attracted great attention due to their inherent characteristics of biocompatibility, nontoxicity and nonantigenicity. In addition, a wide variety of therapeutics can be loaded physically in protein nanoparticles [7, 8]. 5-Flourouracil (5-FU), an effective

✉ \*Corresponding Author Email: [shoja\\_sa@modares.ac.ir](mailto:shoja_sa@modares.ac.ir)

Tel: (+98) 21-82883341

Note. This manuscript was submitted on August 25, 2015; approved on November 5, 2015

chemotherapeutic anticancer drug, has been used against colon, breast, ovarian and skin cancers for about 40 years [9]. In its mechanism of action, when 5-FU incorporates into the cellular metabolism, interferes with the maturation of nuclear RNA, limits cell division, which leads to cellular death causing the tumor shrinking [9]. 5-FU can be administered intravenously and orally [9]. The most serious side effects of 5-FU are chest pain, cardiotoxicity, low blood counts and cognitive impairment [10-12]. Therapeutic effects of anticancer drugs such as 5-FU can be improved and their side effects decreased by the use of targeted delivery systems due to effective targeting of tumor tissues [13-15]. The objective of the present study is the optimized preparation and characterization of HSA nanoparticles dual-loaded with 5-FU and SPIONs as a potential drug delivery system for both therapeutic and diagnostic purposes. To obtain an optimum condition for the SPION entrapment efficiency and 5-FU loading, response surface methodology (RSM) using central composite design (CCD) of the experiments was employed. The physicochemical properties of the system prepared under optimum conditions were characterized thoroughly and 5-FU release was evaluated *in vitro*.

## MATERIALS AND METHODS

Iron oxide nanoparticles (8 nm, magnetic fluid) were purchased from PlasmaChem, Germany. Human serum albumin (fraction V, e" 96%), glutaraldehyde (8% (V/V) in water) and 5-Fluorouracil (e" 99%) were obtained from Sigma, Germany. All other reagents were of analytical grade and used as received.

### *Preparation of HSA nanoparticles loaded with SPIONs and 5-FU*

HSA nanoparticles containing SPIONs and 5-FU were prepared by a desolvation technique as described elsewhere [16]. Briefly, 0.2 g HSA in 2.0 mL aqueous solution, titrated to pH 8.2, containing defined concentrations of SPIONs and 5-FU, was converted to nanoparticles by continuous addition of a desolvating agent, ethanol, at the rate of 1.0 mL/min under constant stirring (800 rpm) at room temperature. Subsequently, 120  $\mu$ L of glutaraldehyde aqueous solution was added to induce particle cross-linking and stabilizing. The cross-linking process was performed under constant stirring of the suspension for 6 hours.

### *Optimization of SPION entrapment efficiency and drug loading*

SPIONs concentration ( $X_1$ ), 5-FU concentration ( $X_2$ ), and pH ( $X_3$ ) were found to be the most significant

factors affecting the production process after some preliminary experiments and considered as the main input variables. For the optimization, RSM using CCD of the experiments at five levels (Table 1). RSM is an assembly of statistical and mathematical techniques that are useful for the modeling and analyses of problems when a response of interest is influenced by several variables and the objective is the optimization of this response. Central composite, Box–Behnken and Doehlert designs are among the principal response surface methodologies used in the experimental design. Central composite design (CCD) is the most popular response surface method due to its capability in building the second order response models. Second-order models have several advantages such as: (1) they are very flexible and can take on a wide variety of functional forms and (2) it is easy to estimate the parameters in a second-order model. SPIONs entrapment efficiency (%) and drug loading (%) were considered as the output responses. The values of all factor levels were chosen according to a previous research [17] and several preliminary experiments.

In order to investigate the optimization of SPIONs entrapment efficiency and 5-FU loading in HSA nanoparticles, CCD-RSM was applied to design of the experiments. Twenty experiments were designed by design expert software (DX-7, State-Ease Inc., Version 7.0.0) and conducted (Table 2); eight of them organized in a full factorial design and six experiments were related to axial points. The other six experiments involved repetition of the central design to obtain a good estimate of the experimental error [18].

### *Purification of nanoparticles*

Dual-loaded HSA nanoparticles were separated from unloaded ones by 3 cycles of centrifugation (30,000  $\times$  g, 10 min) with redispersion of the pellet to the original volume in 10 mM NaCl. Each redispersion step was carried out using ultrasonication (dr. Hielscher, UP 400S, Germany) of the samples. Then, HSA nanoparticles loaded with SPIONs and 5-FU were freeze-dried to yield the nanoparticles powder.

### *Quantification of SPIONs entrapment efficacy in HSA nanoparticles*

After each experiment, the iron content of the dual-loaded HSA nanoparticles was measured by atomic absorption spectroscopy (VARIAN AA240, USA) using a calibration curve of the SPIONs at different concentrations to determine the entrapment efficiency of SPIONs in HSA nanoparticles. In addition, the saturation magnetization of the SPIONs and SPIONs-loaded HSA nanoparticles, were determined by a vibration sample magnetometer (VSM, Iran).

Table1. Main factors and their levels affect the nanoparticles production process

Independent variables	symbol	(- )-1.732	-1	0	+1	(+ )+1.732
SPIONs concentration (mg/ml)	X <sub>1</sub>	1	1.41	2	2.59	3
5-FU concentration (mg/ml)	X <sub>2</sub>	0.5	0.8	1.25	1.7	2
pH	X <sub>3</sub>	7	7.3	7.75	8	8.2

Table 2. Experimental design and results of the SPION entrapment and 5-FU loading efficiencies into HSA nanoparticles using central composite design

Trial	Coded Factors			Experimental Results	
	X <sub>1</sub>	X <sub>2</sub>	X <sub>3</sub>	SPION entrapment (%)	5-FU Loading (%)
1	2.00	1.25	8.50	35	5.58
2	2.59	0.80	8.20	27.7	7.67
3	2.00	1.25	7.00	28.3	1.6
4	2.00	1.25	7.75	26.8	1.5
5	1.41	1.70	7.30	40.4	2.17
6	2.59	1.70	8.20	20.8	7.2
7	3.00	1.25	7.75	15	0.33
8	2.59	1.70	7.30	11.5	1.95
9	1.41	0.80	7.30	29.2	5.3
10	2.00	1.25	7.75	27	8.8
11	1.41	1.70	8.20	23.5	15.8
12	1.41	0.80	8.20	31	13.9
13	2.00	1.25	7.75	27.5	7.4
14	2.00	1.25	7.75	27.3	16.1
15	2.59	0.80	7.30	21	12
16	2.00	1.25	7.75	27	15.3
17	2.00	0.50	7.75	30.6	11.2
18	2.00	2.00	7.75	25.1	4.5
19	1.00	1.25	7.75	40	3.8
20	2.00	1.25	7.75	26.9	14.1

**Assessment of 5-FU loading in HSA nanoparticles**

In order to determine the 5-FU loading, the resulting supernatant obtained after the centrifugation and separation of HSA nanoparticle in each experiment collected and centrifuged again (for one cycle of 30,000 rpm × 20 min) for the separation of possible free SPIONs. Then the amount of non-entrapped 5-FU was measured spectrophotometrically at 266 nm [19] by the use of a 5-FU standard curve. The nanoparticle content was determined gravimetrically and 5-FU loading was calculated using the equation 1.

$$\text{Drug loading (\%)} = \frac{\text{Weigh of drug in nanoparticles}}{\text{Weight of nanoparticles}} \times 100 \quad (1)$$

**Physicochemical characterization of dual-loaded HSA nanoparticles**

Particle size and polydispersity index (PDI) of the dual-loaded HSA nanoparticles produced under the optimum condition were determined by dynamic light scattering (DLS) using a Malvern Zetasizer 3000HS (Malvern Instrument Ltd., UK). Zeta potential of the nanoparticles was also measured to obtain the surface charge of the particles with the same apparatus.

Measurements on the formulation were done in triplicate and results are presented as mean ± standard deviation (SD).

To verify the morphology of Tmx-HSA NPs, a Transmission electron microscopy (TEM) (PHILIPS, EM300) method was used. TEM examination of dual-loaded HSA nanoparticles was carried out with electron kinetic energy of 300 kV. A drop of well-dispersed nanoparticle suspension was placed on Formvar/carbon 200 mesh copper grid and then dried at ambient condition before its attachment to sample holder of the microscope.

**In vitro drug release study**

A suspension of dual-loaded HSA nanoparticles containing 5-FU placed in a dialysis tube and dipped in 10 mL of a phosphate buffer saline (PBS) medium (pH 7.4, 37 °C) under constant stirring (100 rpm). At predetermined time intervals, the release medium was replaced with 10 mL of the fresh PBS. The withdrawn medium was used for the determination of 5-FU amount released during a period of 100 hour. The results are

expressed as a cumulative percentage of the released drug, which calculated using equation 2.

$$\text{Cumulative drug release (\%)} = \frac{\text{Amount of drug released at time t (mg)} \times 100}{\text{Total amount of drug in nanoparticles (mg)}}$$

### Short and long-time physicochemical stability investigation of dual-loaded HSA nanoparticles

In order to evaluate the short-time storage stability of 5-FU and SPIONs loaded HSA NPs, the prepared samples under optimum conditions were stored in PBS (pH 7.4) at 4°C and 37°C. Physicochemical specifications consisting of particle size, polydispersity index and zeta potential were measured 1, 24, 48, 72 and 96 h after production by DLS. For long-time physicochemical stability investigations, samples of dual loaded-HSA NPs containing 5% (w/w) trehalose as a preservative [20] were freeze-dried and stored at room temperature. The samples were resuspended in distilled water every two weeks and then, analyzed with DLS during a period of 12 weeks.

## RESULTS AND DISCUSSION

### SPION entrapment and drug loading optimization

As described before, 5-FU concentration, SPION concentration and pH were selected as the independent input variables, and the drug loading and SPION entrapment efficiencies as the dependent output variables. According to several preliminary experiments, the lowest and the highest levels of the drug and SPION concentrations were determined.

A central composite design was employed to analyze the interactive effects of these parameters and to arrive at an optimum condition. A 2<sup>3</sup>-factorial central composite experimental design, with six axial points and six replications at the center point leading to a total number of 20 experiments was carried out for the optimization of the parameters. The variables were coded according to the following equation:

$$X_i = (x_i - x_i^*) / \Delta x_i$$

Where  $X_i$  is the coded value,  $x_i$  is the actual value of the  $i$ th test variable,  $x_i^*$  is the value of  $x_i$  at the centre point of the investigated area, and  $\Delta x_i$  is the step size. The range of the variables is given in Table 1. The experimental design protocols developed by DX-7 and corresponding results are presented in Table 2.

The experimental results of the CCD were fitted with a second-order polynomial equation. The values of regression coefficients were calculated and the fitted equations (in terms of coded values) for prediction of

the maximum entrapment of the SPIONs and 5-FU loading were as follows, respectively:

$$Y_1 = +27.19 - 7.13 X_1 - 2.43 X_2 - 8.67 \times 10^{-4} X_3 - 0.99 X_3 X_2 + 5.41 X_1 X_3 - 0.49 X_2 X_3 - 0.26 X_1^2 - 0.24 X_2^2 + 1.21 X_3^2 \quad (3)$$

$$Y_2 = +152 + 1.71 X_1 + 0.17 X_2 + 1.23 X_3 + 0.11 X_1 X_2 + 1.63 X_1 X_3 - 0.31 X_2 X_3 - 1.85 X_1^2 + 3.31 X_2^2 + 0.52 X_3^2 \quad (4)$$

Where  $Y_1$  and  $Y_2$  are the SPION entrapment and 5-FU loading efficiencies, respectively.  $X_1$ ,  $X_2$ , and  $X_3$  are coded values of SPION concentration, the drug concentration and pH, respectively.

The coefficients of the regression models that appear at one constant, three linear, three quadratic, and three interaction terms are listed in Tables 3 and 4. The  $P$ -value, which determines the significance of each value, is also given.

SPION concentration was found to have the most significant main effect. The SPION concentration-pH term was found to be the most significant term in interactions. Likewise, in equation 4,  $P$ -values imply that the first order main effects, namely SPION concentration and pH, and the second order main effects of all three variables are significant in 5-FU loading. It is noteworthy that the most significant second order term is for 5-FU concentration with the  $P$ -value < 0.0001. The interaction term, 5-FU concentration-pH, is also significant. Therefore, they can act as limiting factors and small variations in their amount will alter nanoparticle production with the desired SPION entrapment efficiency (%) and 5-FU loading (%). It is required to test the significance and adequacy of the model through analysis of variance. The analysis of variance of the regression model demonstrates that the model is highly significant, as is evident from the Fisher's  $F$  test.  $F$  model equals 12.08 and 20.93 for the SPION entrapment efficiency (%) and 5-FU loading (%), respectively. The goodness of the fit with this quadratic model was confirmed by the determination coefficient ( $R^2$ ).

In this case, the value of the determination coefficient indicates that the model can explain 92.36% and 96.42% for the variability in the responses of the SPION entrapment efficiency and 5-FU loading, respectively. The optimum conditions were found to be pH 8.2, SPION concentration 2.79 mg/mL and 5-FU concentration 1.5 mg/mL. The optimal SPION entrapment efficiency of 40.42% and 5-FU loading efficiency of 16.89% were predicted by the software for the production of dual-loaded HSA nanoparticles.

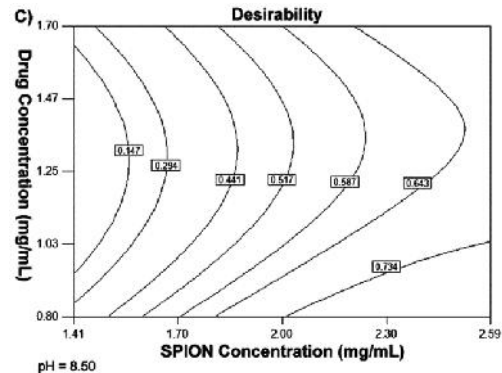
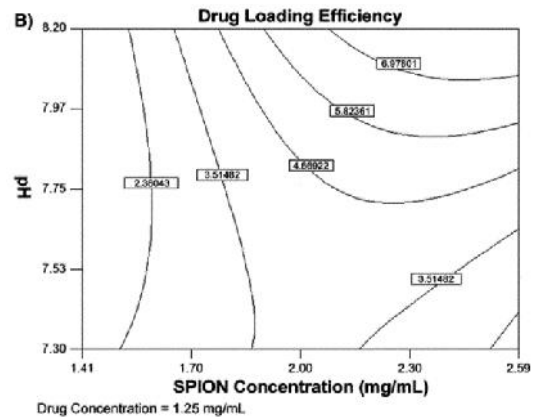
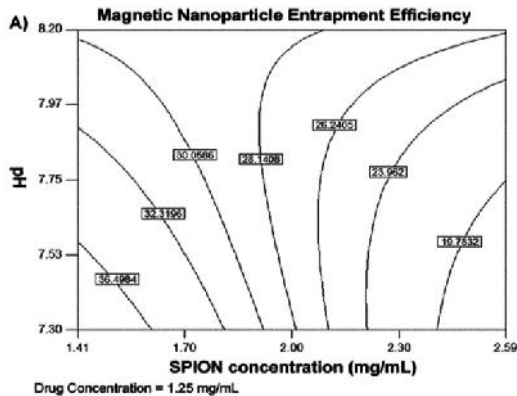
Table 3. ANOVA Table for the SPION entrapment efficiency

Source	Sum of squares	Df	Mean square	F-value	P-value prob >F
Model	844.75	9	93.86	12.08	0.0005
A	567.70	1	567.70	73.07	<0.0001
B	65.75	1	65.75	8.46	0.0173
C	8.421E-006	1	8.421E-006	1.084E-006	0.999
AB	5.69	1	5.69	0.73	0.4144
AC	169.85	1	169.85	21.86	0.0012
BC	1.39	1	1.39	0.18	0.6819
A <sup>2</sup>	0.95	1	0.95	0.12	0.7351
B <sup>2</sup>	0.82	1	0.82	0.11	0.7523
C <sup>2</sup>	20.38	1	20.38	2.62	0.1398

Table 4. ANOVA Table for the 5-FU loading efficiency

Source	Sum of squares	Df	Mean square	F-value	P-value (prob >F)
Model	161.55	9	17.95	20.93	0.0003
A	14.75	1	14.75	17.20	0.0043
B	0.14	1	0.14	0.17	0.6957
C	14.56	1	14.56	16.98	0.0045
AB	0.056	1	0.056	0.066	0.8048
AC	12.51	1	12.51	14.59	0.0065
BC	0.46	1	0.46	0.54	0.4878
A <sup>2</sup>	21.66	1	21.66	25.26	0.0015
B <sup>2</sup>	69.25	1	69.25	80.76	<0.0001
C <sup>2</sup>	3.67	1	3.67	4.28	0.0774

Confirmation experiments under the optimum condition were conducted in triplicate and average values of 41.1% and 15.8% were acquired for the SPION entrapment efficiency and drug loading, respectively. The good agreement between these predicted and experimental results confirms the validity of the models. Contour plots generated from the predicted data illustrate the effect of each pair of independent variables on the optimization of the SPION entrapment efficiency and 5-FU loading (Fig. 1). Two-dimensional contour plots are the graphical presentation of the regression equation and are plotted to understand the interaction of the variables and to locate the optimum level of the two variables corresponding to the maximum response.



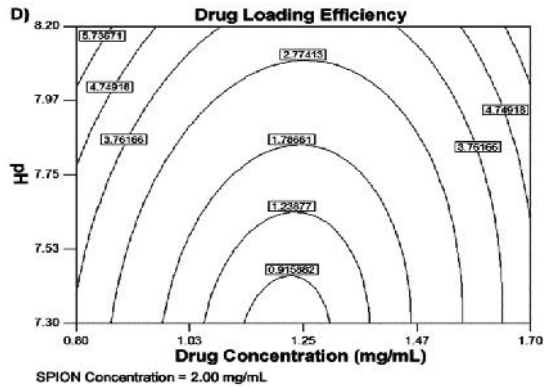


Fig. 1. Contour plots a) pH-SPION interaction, b) pH-SPION interaction, c) 5-FU concentration-SPION concentration interaction, d) 5-FU concentration-pH interaction

### Particle size and zeta potential of dual-loaded HSA nanoparticles

Average diameter and zeta potential of dual-loaded HSA nanoparticles, synthesized under optimum condition was  $111.8 \pm 14$  nm and  $-37.1 \pm 3.1$  mV, respectively. In order to evaluate the short- and long-term storage stability, the drug and SPIONs loaded nanoparticles were prepared under optimum conditions as described earlier. For short-term stability experiments, the samples were stored at 4 and 37 °C for a period of 96 h. The results revealed that average size, PDI and zeta potential did not change significantly at both 4 °C and 37 °C during all time intervals of the storage. These results indicate that the short-term storage of nanoparticles at both 4 °C and 37 °C for 96 h do not change significantly the physicochemical properties of nanoparticles and, therefore can be considered as the conditions for short time storage.

For long-term stability experiments, the samples of nanoparticles prepared under optimum conditions and containing 5% trihalose were initially freeze-dried and then maintained at room temperature. The physicochemical properties of nanoparticles were measured every two weeks by DLS for a storage period of 12 weeks. A little growth in particle size observed after 12 weeks of storage due to the particles adherence, but the size is still in acceptable range for use as a delivery system (Table 5). Therefore, Freeze-drying of nanoparticles can preserve the properties of nanoparticles. The long time stability of powder form of dual-loaded nanoparticles make them attractive as a targeted delivery system.

### Transmission Electron Microscopy

As described earlier, TEM was used to study the entrapment and distribution of the SPIONs within the HSA nanoparticles. The TEM image (Fig. 2) clearly confirms the spherical shape of nanoparticles and successful entrapment of SPIONs in the polymeric matrix.

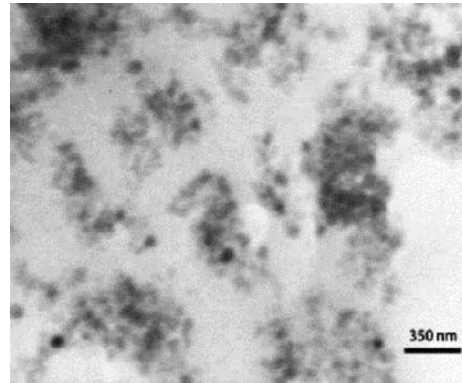


Fig. 2. TEM image of the produced dual-loaded nanoparticles under optimum conditions

### In vitro drug release

5-FU release from dual-loaded HSA nanoparticles was conducted as described earlier. The cumulative release profile is presented in Fig. 3. In this Fig the y-axis is the cumulative percentage of the released 5-FU, and the x-axis is time. This Fig exhibits that in the early hours of release there exists a burst effect, which is most probably because of the 5-FU adsorbed on the HSA nanoparticles. This initial fast release is in accordance with our previous observations [19, 21]. Controlled release of the drug in the following hours shows that this system can release the drug in a sustained controllable manner that is convenient for a drug delivery system.

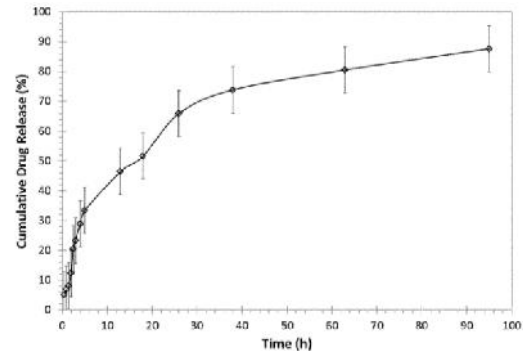


Fig. 3. In vitro cumulative release of 5-FU in PBS, pH 7.4 and temperature 37 °C

Table 5. Long-term stability investigation of physicochemical characteristics of dual-loaded HSA nanoparticles

Parameters	Unloaded HSA nanoparticles		Dual-loaded nanoparticles	
	Right after synthesis	After 12 weeks	Right after synthesis	After 12 weeks
Particle size (nm)	97.5±6	99.1±12	111.8±14	138.4±21
Zeta potential (mV)	-31.7±2.4	-32.1±3.3	-37.1±3.1	-38.2±4
PDI	0.049	0.068	0.064	1.023

**Saturation magnetization measurements**

Characteristics of the hysteresis loops and field-dependent magnetizations at constant temperature were evaluated for dual-loaded HSA nanoparticles in comparison with the SPIONs. Figure 4 shows VSM measurement of magnetization of the SPIONs and the dual-loaded HSA nanoparticles at 300 K. This Fig reveals that, in general, these two entities display similar magnetic behavior. They show superparamagnetic characteristics with no hysteresis cycle. Therefore, it can be concluded that SPIONs-loaded HSA nanoparticles maintain the superparamagnetic properties of the SPIONs. As shown in this Fig, by the SPIONs entrapment into HSA nanoparticles, the magnetization shows a reduction and it is because of the protein layer around the magnetic nanoparticles that affect the surface characteristics of the SPIONs [22, 23].

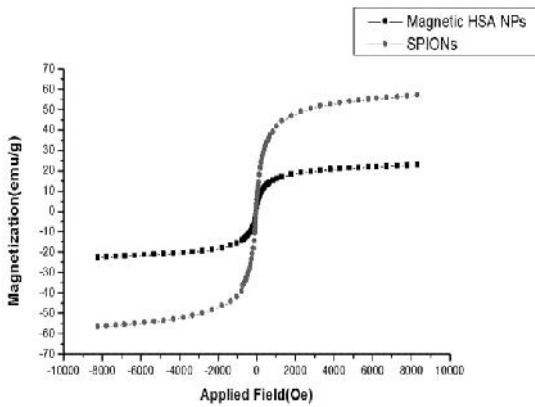


Fig. 4. Magnetization measurement of SPIONs and dual-loaded HSA nanoparticles

**CONCLUSION**

In this study, an optimum production process for dual-loaded HSA nanoparticles with superparamagnetic properties was investigated. The nanoparticulate system was prepared by the ethanolic desolvation technique. The effect of significant process variables on the production of SPIONs and 5-FU loaded albumin nanoparticles was evaluated, and the optimum condition was determined by CCD-RSM.

A 2<sup>3</sup>-factorial central composite design, with six axial points and six replications at the center point leading to a total number of 20 experiments carried out for the optimization of the parameters. Optimum conditions predicted to be pH 8.2, drug concentration of 1.5 mg/ml and SPION concentration of 2.79 mg/ml. 5-FU loading and SPION entrapment efficiency of 15.8% and 41.1% achieved, respectively. Under these conditions, dual-loaded nanoparticles with the average radius of 111.8 nm, zeta potential of -37.1 mV and PDI of 0.064 produced. Confirmation experiments carried out in triplicate and the obtained results confirmed the predicted optimum condition by the DX-7 software. Transmission electron microscopy (TEM) indicated that SPIONs entrapped into the protein matrix of HSA

*In vitro* cumulative release of 5-FU from magnetic HSA nanoparticles was evaluated in PBS solution, pH 7.4 at 37 °C. 5-FU released totally after 93 hours, which indicates an appropriate control over drug release by the nanoparticulate system at sink condition. In addition, Vibrating Sample Magnetometer (VSM) analysis showed that the produced magnetic albumin nanoparticles under optimum condition had superparamagnetic property, providing magnetic targeting ability to the drug carrier system. Stability investigations were conducted by storing the nanoparticulate system for 12 weeks. After this time, the change in physicochemical properties was negligible. In conclusion, according to the findings, SPIONs and 5-FU loaded HSA nanoparticles are promising for use as a novel targeted delivery system due to proper magnetic and drug release behaviours.

**ACKNOWLEDGMENTS**

The financial support from Shahaid Behashti University and Tarbiat Modares University, Tehran, Iran are greatly acknowledged.

**REFERENCES**

[1] Sun C, Lee JSH, Zhang M. Magnetic nanoparticles in MR imaging and drug delivery. *Adv Drug Delivery Rev.* (2008)1252-60: 1252-1265.  
 [2] Mohammad-Taheri M, Vasheghani-Farahani E, Hosseinkhani H, Shojaosadati SA, Soleimani M.

- Fabrication and characterization of a new MRI contrast agent based on a magnetic dextran-spermine nanoparticles. *Iran J Polym Sci Technol.* (2012)21: 239-251.
- [3] Chertok B, Moffat B.A, David A.E, Yu F, Bergemann C, Ross BD, Yang VC. Iron oxide nanoparticles as a drug delivery vehicle for MRI monitored magnetic targeting of brain tumors. *Biomaterials.* 2008; 29: 487-496.
- [4] Kumar CSSR, Mohammad F. Magnetic nanomaterials for hyperthermia-based therapy and controlled drug delivery. *Adv. Drug Delivery Rev.* 2011; 63: 789-808.
- [5] Laurant S, Dutz S, Hafeli U.O, Mahmoudi M. Magnetic fluid hyperthermia: Focus on superparamagnetic iron oxide nanoparticles. *Adv Colloid Interface Sci.* 2011; 166: 8-23.
- [6] Pouponeau P, Leroux JC, Soulez G, Gaboury L, Martel S. Co-encapsulation of magnetic nanoparticles and doxorubicin into biodegradable microcarriers for deep tissue targeting by vascular MRI navigation. *Biomaterials.* 2011; 32: 3481-3486.
- [7] Kratz F. Albumin as a drug carrier: Design of prodrugs, drug conjugates and nanoparticles. *J. Controlled Release.* 2007; 132: 171-183.
- [8] Wacker M, Zensi A, Kufleitner J, Ruff A, Schütz J, Stockburger T, Marstaller T, Vogel V. A toolbox for the upscaling of ethanolic human serum albumin (HSA) desolvation. *Int. J. Pharm.,* 2011; 46: 225-232.
- [9] Longley DB, Harkin DP, Johnston P.G. 5-Fluorouracil: mechanisms of action and clinical strategies. *Nat. Rev. Cancer,* 2003; 3: 330-338.
- [10] Pinedo HM, Peters GF. Fluorouracil: biochemistry and pharmacology *J Clin Oncol.* 1988; 6: 1653-1664.
- [11] Alter P, Herzum M, Soufi M, Schaefer JR, Maisch B. Cardiotoxicity of 5- fluorouracil. *cardiovasc Hematol Agents Med Chem.* 2006; 4(1): 1-5.
- [12] Wigmore PM, Mustafa S, El-Beltagy M, Lyons L, Umka J, Bennett G. Effects of 5-FU. *Adv Exp Med Biol.* 2010; 678: 157-164.
- [13] Fadeian G, Shojaosadati SA, Kouchakzadeh H, Shokri F, Soleimani M. Targeted Delivery of 5-fluorouracil with Monoclonal Antibody Modified Bovine Serum Albumin Nanoparticles. *Iranian J Pharm Res.* 2015; 14(2) 395-405.
- [14] Kouchakzadeh H, Shojaosadati SA, Mohammadnejad J, Paknejad M, Rasaei MJ. Attachment of an anti-MUC1 monoclonal antibody to 5-FU loaded BSA nanoparticles for active targeting of breast cancer cells. *Hum Antibodies.* 2012; 21: 49-56.
- [15] Danhier F, Feron O, Preat V. To exploit the tumor microenvironment: passive and active tumor targeting of nanocarriers for anti-cancer drug delivery. *J Control Release* 2010; 148(2): 135-146.
- [16] Langer K, Balthasar S, Vogel V, Dinauer N, von Briesen H, Schubert D. Optimization of the preparation process for human serum albumin (HSA) nanoparticles. *Int J Pharm.* 2003; 257 (1-2): 169-180.
- [17] Pouponeau P, Leroux JC, Martel S. Magnetic nanoparticles encapsulated into biodegradable microparticles steered with an upgraded magnetic resonance imaging system for tumor chemoembolization. *Biomaterials.* 2009; 30: 6327-6332.
- [18] Kouchakzadeh H, Shojaosadati SA, Shokri F. Efficient loading and entrapment of tamoxifen in human serum albumin based nanoparticulate delivery system by a modified desolvation technique. *chem eng res des.* 2014; 92: 1681-1692.
- [19] Maghsoudi A, Shojaosadati SA, Vasheghani-Farahani E. 5-Fluorouracil-Loaded BSA Nanoparticles: Formulation Optimization and In Vitro Release Study. *AAPS PharmSciTech.* 2008; 9: 1092-1096.
- [20] Anhorn MG, Mahler HC, Langer K. Freeze drying of human serum albumin (HSA) nanoparticles with different excipients. *Int. J. Pharm.* 2008; 363: 162-169.
- [21] Kouchakzadeh H, Shojaosadati SA, Maghsoudi A, Vasheghani Farahani E. Optimization of PEGylation conditions for BSA nanoparticles using response surface methodology. *AAPS PharmSciTech.* 2010; 11: 1206-1211.
- [22] Calatayud MP, Sanz B, Raffa V, Riggio C, Ibarra MR, Goya GF. The effect of surface charge of functionalized Fe<sub>3</sub>O<sub>4</sub> nanoparticles on protein adsorption and cell uptake. *Biomaterials.* 2014; 35: 6389-6399.
- [23] Issa B, Obaidat IB, Albiss BA, Haik Y. Magnetic Nanoparticles: Surface Effects and Properties Related to Biomedicine Applications. *Int J Mol Sci.* 2013; 14: 21266–21305.

**How to cite this article:**

Kouchakzadeh H, Hoseini Makarem S, Shojaosadati SA. Simultaneous loading of 5-fluorouracil and SPIONs in HSA nanoparticles: Optimization of preparation, characterization and *in vitro* drug release study. *Nanomed. J.*, 2016; 3(1): 35-42.

DOI:10.7508/nmj.2016.01.004

URL:[http://nmj.mums.ac.ir/article\\_6194\\_888.html](http://nmj.mums.ac.ir/article_6194_888.html)